Non Equilibrium Plasma Flows in a Low-pressure Supersonic Arcjet Facility

D. LeQuang[1,2], *M. Lino da Silva*[1], *and M. Dudeck*[2]

(1): Instituto de Plasmas e Fusão Nuclear, Instituto Superior Técnico, Av. Rovisco Pais, 1049–001, Lisboa, Portugal
(2): Université Pierre et Marie Curie Paris VI, 4 Place Jussieu, 75005 Paris, France
mlinodasilva@mail.ist.utl.pt/Fax: +351 21 841 44 55

Abstract

The internal levels populations of the radiating species in the exit of a low-pressure, supersonic D. C. arc-jet plasma generator have been investigated, for Martian, Earth and Titan-like mixtures A 1D stationary hydrodynamic model, taking into account a Landau-Teller model for the relaxation of the internal modes has been firstly utilized to calculate the temperatures in the arc-jet nozzle throat and diverging region. The simulated temperatures have then been compared against experimentally-determined temperatures at the nozzle exit, obtained through the line-by-line fitting of experimental spectra. The obtained results show that the numerical simulations predict reliable rotational temperatures. This is no longer the case for vibrational levels populations, which are found not to follow a Boltzmann-like distribution.

1 Introduction

Planetary exploration in the solar system requires high accuracy codes to model the plasma flow surrounding a spacecraft during its hypersonic-supersonic flight (at velocities up to 11km/s) in the upper layers of a planetary atmosphere. Theses codes are essential to estimate the energy fluxes impacting the surface of the spacecraft allowing the optimization of its thermal protection system (TPS). However, new trajectories including for exemple: aerobraking or aerocapture of the spacecraft, require codes giving results precise enough to start a space mission. These codes are complex due to the number of phenomena to be inserted (convective effects, transport effects, dissociation, ionization, optical emission in a large wavelength range, cathalicity effects) and imperatively ask validated data. They are also related to a specific planetary atmosphere, with each planetary having a particular atmosphere with a different gas composition and different thermodynamical properties in the temperature and pressure ranges. Such codes are typically developed in correlation with experiments carried out in ground test facilities such as shock tubes, microwave sources, inductively plasma torches (ICP) and arc-jets. A D.C. arc-jet facility is used in the ICARE laboratory to simulate the plasma conditions appearing around a spacecraft during its descent in a planetary atmosphere. Different gas compositions as CO2-N2 (Mars simulation), N2-O2 (Earth simulation) and N2-CH4 (Titan simulation) are considered as a working gas for this facility. A 1D code (TNeC) has been developed to estimate the evolution of the translational - rotational - vibrational temperatures in the arc-jet for the three gases and the behavior of these temperatures and their non equilibrium evolutions using a Landau-Teller law for the rotational and vibrational relaxations are presented in this paper. These temperatures are estimated for same total mass flow rate and input energy in the throat of the nozzle. Optical emission spectroscopy is a useful non intrusive tool allowing an analysis of the non equilibrium plasma conditions. An optical spectrometer for near VUV-near IR has been used to characterize the plasma flow at the exit of the arc-jet and the recorded spectra have been compared with calculated spectra obtained with the code SPARTAN to estimate the rotational and the vibrational temperatures.

2 Experimental Facility and Tools for the Modelling of Plasma Processes and Properties

2.1 The SR5 Arc-jet Plasma Facility

The SR5 low pressure arc-jet plasma wind tunnel available at the Laboratoire ICARE is a facility dedicated to the study of low pressure, high temperature plasmas, typical of an atmospheric entry. The facility is composed of a 4.3 m long and 1.1 m diameter vacuum chamber, coupled to a pumping system of 26000 $m^3\ h^{-1}$ capacity which ensures an ambient chamber pressure of about 2-10 Pa.

Fig. 1: Supersonic plasma wind tunnel facility

A D.C. vortex-stabilized arc discharge is generated between the tip of a cathode, which is a small zirconium disk inserted into copper (disk diameter 1.6 mm), and the nozzle throat, which operates as the anode (cylindrical neck of 4 mm length and 4 mm internal diameter, made of tungsten inserted into copper). The arc operates at low voltages (50–100 V) and low currents (50–150 A) delivering typical powers of 5–10 kW to the flow in the throat region of the nozzle. A low mass-flow rate (0.1–0.5 g/s) is supplied to the nozzle, which allows obtaining a high-enthalpy (5–30 MJ/kg) steady plasma jet with a global yield of 50-70%. The arc discharge is ignited through a high frequency, high voltage pulse (1 MHz - 4000 V). Different plasma mixtures, simulating various planetary atmospheres (Earth, Mars, Titan) have been successfully obtained in this facility, as the zirconium anode and cathode allow reproducing stable plasma flows even with oxygen containing chemical mixtures. Copper pieces, anode as well as cathode are water cooled. Balance energy on inlet and outlet water circuit temperatures, measured by thermocouple's, is used to determine the efficiency of the plasma generator. The diverging section of the nozzle is 53 mm long with an exit diameter of 48 mm which corresponds to a 25.4 ° half-angle.

A schematic view of the nozzle is presented in Fig. 2.

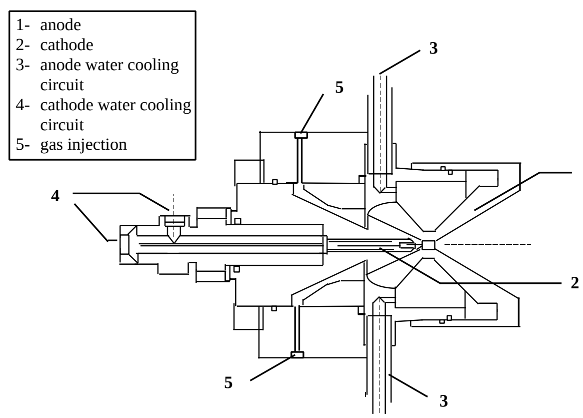

Fig. 2: SR5 nozzle scheme

Spectral measurements were carried using a SOPRA F1500 (Ebert-Fastie type) monochromator with a focal length of 1500 mm and a grating of 1800 grooves/mm sweeping a spectral region from 2700 Å in the near-ultraviolet region to 950 Å in the near-infrared region. The grating is connected to an intensified optical multichannel analyzer (Princeton Instruments IRY 1024). This device allows a 85-Å wavelength region to be expanded on 1024 pixels and is cooled by a Peltier element insuring an operating temperature of -35°C. The plasma is imaged onto the monochromator by a mirror telescope connected to the entrance slit by a quartz optical fiber. The entrance slit opening can be adjusted, therefore modifying the experimental apparatus function which can reach values down to a full width at half maximum (FWHM) of 0.25 Å. Such optical setup is held in a fixed position, with a robotic arm allowing for the movement of the plasma source in the axial and vertical planes. This allows the easy optical probing of the overall plasma plume. The optical setup is presented in Fig. 3

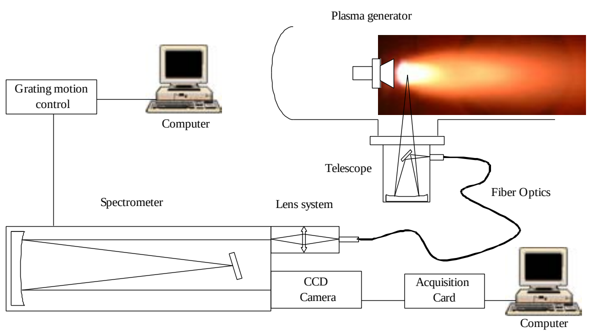

Fig. 3: Optical spectrometry set-up scheme

Local spectra is retrieved through the measurement of spectral properties every 2.5mm from the plasma jet axis, up to the point where a signal is no longer retrieved. Then the Abel Inversion technique is applied, and a local spectra is then retrieved. The example of the Abel inversion technique, applied to the CN Violet spectrum in a N_2–CH_4 plasma, is presented in Fig. 4

2.2 Line-by-Line Modelling of the Plasma Emission Spectra

The SPARTAN code [1, 2] is a Line-by-Line code tailored for the simulation of radiation from low-pressure plasmas, with an emphasis on atmospheric entry applications. The code and its associated radiative database encompasses around 60 bound, bound-free and free radiative transitions from more than 20 chemical species ranging from the VUV to the IR

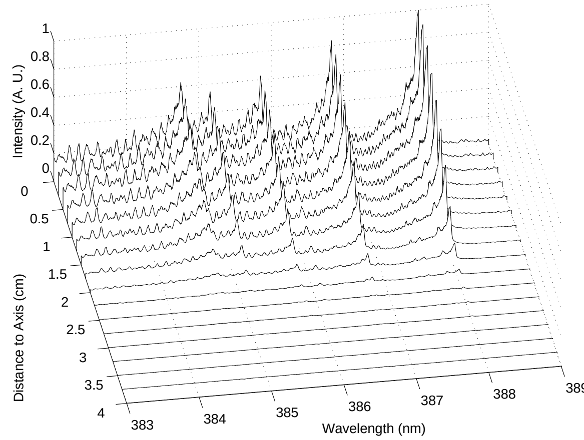

Fig. 4: Example of an Abel Inversion in the nozzle exit region, for a N_2–CH_4 mixture

region. The lineshape routine of the code considers a Voigt line profile, accounting for the effects of Doppler, but also collisional (collisional, ressonance, Van der Waals, Stark) broadening processes.

The associated spectral database has been properly tailored for the simulation of radiative transitions encountered in Air and CO_2–N_2 plasmas. Accurate spectroscopic constants from different bibliographical resources have been imputed in a numerical routine which reconstructs the potential curves for the transition electronic states using an RKR method and calculates the upper and lower states wavefunctions solving the radial Schrödinger equation. Such wavefunctions are then coupled to accurate electronic transition moments from the literature, to yield appropriate Einstein coefficients [3].

The code considers the traditional approximation of a Boltzmann equilibrium distribution for the internal levels populations, with the specificity that thermal nonequilibrium in the population of the different internal modes can be considered, accounting for a single translational temperature T_{tr}, and species dependent rotational, vibrational and electronic excitation temperatures $(T_r, T_v, T_{exc})_i$. In case a Non-Boltzmann distribution of the internal atomic and molecular levels needs to be considered, the code allows inputting custom population distributions for the internal electronic and vibrational levels. This method allows reproducing experimentally measured non-Boltzmann distributions through the trial-and-error fitting of experimentally-determined spectra by synthetic spectra.

2.3 Nozzle Flow Modelling Using a Multitemperature Model

The hydrodynamic modelling of nozzle flows is a quite challenging task. Typically the generator conditions of the plasma in the discharge region are unknown, as probing them through experimental techniques is quite difficult. Usually, the earliest location where experimental measurements can be carried out is the nozzle exit, if we consider non-intrusive optical diagnostics [4, 5, 6], or even farther in the flow, if we consider intrusive diagnostics like electrostatic probes. One is usually limited to defining a simplified model in the arc region, and this is what has been done in a previous work, which considered a 1D constant-heat addition of energy by the arc in the nozzle throat region [7]. The same simplified quasi-1D model, developed as the *TNeC* code has been considered in this work, as it is properly tailored for the detailed simulation of energy exchange processes between the translational and internal modes of the plasma molecules [7].

The capabilities of the *TNeC* code are as follows: Forward and backward chemical reaction rates from any arbitrary chemical dataset are considered using the Arrhenius law; V–D coupling is taken into account considering a nonequilibrium factor calculated according to the relation proposed by Shatalov and Losev [8], with the possibility of using the more simplified Park model [9]; Energy exchange processes between the internal modes of the different species are taken into account; Rotational and vibrational relaxation modes for each molecule are solved in the usual way using Landau-Teller relation [10]; Rate coefficients for V–T and V–V processes are issued from the expressions of Millikan&White [11] updated by Park [12] for N_2–O_2 mixtures, and from Losev [13] for CO_2–N_2 mixtures.

For other mixtures such as Titan-like N_2–CH_4 flows, relaxation times have to be arbitrarily approximated due to the lack of appropriate datasets. In the scope of this study, we have worked with the following approximations:

$$\tau_{X-N_2} = \tau_{X-H_2} = \tau_{X-NH} = \tau_{X-CH} = \tau_{X-CH_x} \quad (1)$$

$$\tau_{X-O_2} = \tau_{X-C_2} = \tau_{X-CN} \quad (2)$$

For R–T coupling, the Z_R coefficient is taken as 15.7 for N_2 and 14.4 for O_2, according to Parker [10]. Overall, the database respectively encompasses 121, 72 and 24 V–T, 44, 30 and 12 V–V, 100, 54 and 16 R–T processes for CO_2–N_2, O_2–N_2 and N_2–CH_4 mixtures. For a Martian-like gas mixture, the species taken into account in the TNeC code are: C, N, O, C_2, N_2, O_2, CO, CN, NO and CO_2. For a Titan-like mixture, the species taken into account are: H, C, N, N_2, C_2, H_2, CH, CN, NH, CH_2, CH_3 and CH_4. For an Air mixture, the species taken into account are: N, O, N_2, O_2, and NO. The selected chemical reactions are issued form Park for Air [12] and CO_2–N_2 plasmas [14], and from Gokcen for N_2–CH_4 plasmas [15]. A more complete description of this code can be found in [4].

3 Comparison of Experimentally-Determined Level Populations With Calculation Results

Two complementary investigations have been carried out. Firstly, the influence of the plasma chemical composition on the properties of a species emission spectra has been investigated. For this, we have investigated the CN Violet spectrum at the nozzle exit, for two different plasma mixtures: a CO_2–N_2 and a N_2–CH_4 plasma. Secondly, the arc power budget influence on the emission spectra of an ionized species has been investigated. In this second case, we have examined the First Negative spectrum of N_2^+ for an Air plasma with varying arc power input. The plasma operation parameters are presented in Tab. 1 for a 90%CO_2–10%N_2 flow, Tab. 2 for a 95%N_2–5%CH_4 flow, and Tab. 3 for a 80%O_2–20%N_2 flow.

The quasi-1D numerical code has firstly been applied to the reproduction of the SR5 nozzle flow for

CO_2N_2 Plasma Parameters			
$\dot{m}_{CO_2}$	8.9 slm	ΔE_{arc}	+ 6.65 kW
$\dot{m}_{N_2}$	0.99 slm	$\Delta E_{cathode}$	– 0.44 kW
$\dot{m}$	0.31 g/s	ΔE_{anode}	– 2.68 kW
$P_{generator}$	32530 Pa	h_{gas}	11.4 MJ/kg
$P_{chamber}$	5.3 Pa	η	47 %

Tab. 1: Facility Operating Characteristics for a Martian-like Plasma

N_2–CH_4 Plasma Parameters			
$\dot{m}_{N_2}$	28.5 slm	ΔE_{arc}	+ 5.43 kW
$\dot{m}_{CH_4}$	1.5 slm	$\Delta E_{cathode}$	– 0.64 kW
$\dot{m}$	0.45 g/s	ΔE_{anode}	– 2.23 kW
$P_{generator}$	49328 Pa	h_{gas}	3.5 MJ/kg
$P_{chamber}$	5.3 Pa	η	53 %

Tab. 2: Facility Operating Characteristics for a Titan-like Plasma

N_2–O_2 Plasma Parameters					
Main Input	$\dot{m}_{N_2}$	15.92 slm	Input Power Case 3	ΔE_{arc}	+ 6.97kW
	$\dot{m}_{O_2}$	3.98 slm		$\Delta E_{cat.}$	– 0.64kW
	$\dot{m}$	0.40 g/s		$\Delta E_{an.}$	– 2.17kW
	$P_{gen.}$	39900Pa		h_{gas}	10.4MJ/kg
	$P_{chamb.}$	5.3Pa		η	59 %
Input Power Case 1	ΔE_{arc}	+ 4.25kW	Input Power Case 4	ΔE_{arc}	+ 8.63kW
	$\Delta E_{cat.}$	– 0.32kW		$\Delta E_{cat.}$	– 0.64kW
	$\Delta E_{an.}$	– 1.81kW		$\Delta E_{an.}$	– 2.71kW
	h_{gas}	5.3 MJ/kg		h_{gas}	13.2MJ/kg
	η	49 %		η	61%
Input Power Case 2	ΔE_{arc}	+ 5.15kW	Input Power Case 5	ΔE_{arc}	+ 10.4kW
	$\Delta E_{cat.}$	–0.32kW		$\Delta E_{cat.}$	– 0.64kW
	$\Delta E_{an.}$	– 1.63kW		$\Delta E_{an.}$	– 3.26kW
	h_{gas}	7.9 MJ/kg		h_{gas}	16.2MJ/kg
	η	62 %		η	62 %

Tab. 3: Facility Operating Characteristics for a Air Plasma

these three different chemical mixtures. Among the different parameters that the numerical code can provide, we have selected the different species translational and internal temperatures at the nozzle axis, which yield information on these species internal levels populations. As explained in detail in Ref. [7], the flow in the nozzle throat is firstly calculated, providing inlet conditions for the calculation of the plasma flow in the nozzle diverging region.

3.1 Comparison of Measured and Simulated CN Populations for a Martian-like and a Titan-like Plasma

The comparison of the first two CN-containing plasmas is presented in Figs. 5 and 6, respectively for a CO_2–N_2 and a N_2–CH_4 plasma.

For the CO_2–N_2 plasma, with an arc power of 6.6kW and an average enthalpy of 11.4MJ/kg, the gas temperature T linearly increases at to the middle part of the throat before to take into account endothermic chemical processes and reach a value around 8,500K at the throat exit. The rotational temperature T_r follows closely the translational temperature T, as a result of the efficiency of T–R processes and the relatively high densities reached in the nozzle throat. The vibrational temperatures T_v follow the increase of the translational temperature T more slowly, as a result of the less efficient T–V exchanges, and depending on the individual relaxation times of the different molecular species, which range from 4,500K to 6,000–8,500K for the different species.

In the divergent section of the nozzle the translational temperature T decreases due to the pressure decrease, reaching a final value around 2,500K in the nozzle exit. The increasing rarefaction effects in the nozzle diverging region lead to a decrease in the T–R exchanges, with the consequence that the different species rotational temperatures slowly stop relaxing, diverging from the translational temperature T. Although a total freezing of the rotational temperature is not achieved in the simulation, the different rotational temperatures remain at a value significantly above the translational temperature T, at values around 4,500–4,850K. As regarding vibrational temperatures, they start freezing more quickly, as it would be expectable.

For the N_2–CH_4 plasma, with an arc power of 5.4kW and an lower average enthalpy of 3.5MJ/kg,

the translational temperature T presents a particular behavior, showing a plateau between 1.5 and 3mm due to the strong endothermic dissociation reactions of CH_4, which are initiated as soon as the translational temperature exceeds 2,000K. CH_4 is fully dis-

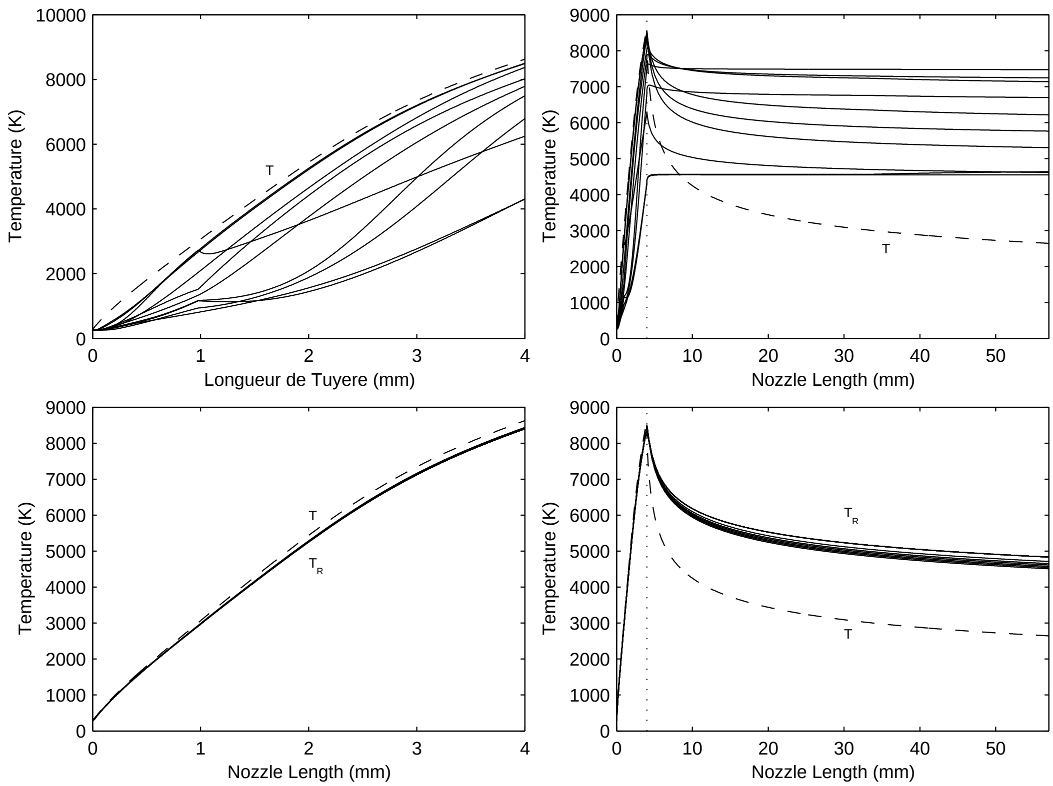

Fig. 5: Vibrational (Top) and Rotational (Bottom) Temperatures of the Molecular Species in the Nozzle Throat (Left) and Diverging Section (Right), for a CO_2–N_2 Mixture

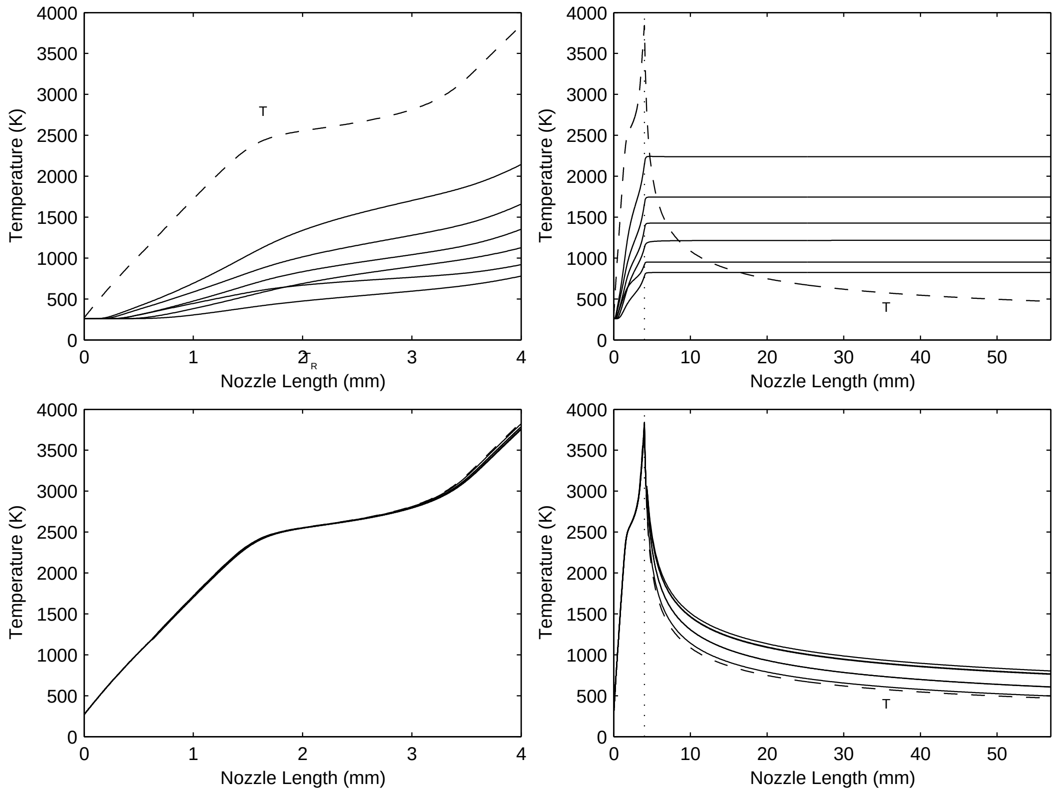

Fig. 6: Vibrational (Top) and Rotational (Bottom) Temperatures of the Molecular Species in the Nozzle Throat (Left) and Diverging Section (Right), for a N_2–CH_4 Mixture

sociated to form successively CH_3, CH_2 and finally CH. At the nozzle throat exit, the remaining species are mostly N_2, CH and H. The plot for the evolution of the molar fractions in the nozzle throat is presented in Fig. 7. The translational temperature at the throat exit is only T=3,800K with, as always, an equilibrium with the rotational temperature T_r. Relaxation processes proceed similarly to the CO_2–N_2 plasma, with the difference that vibrational temperatures are instantaneously frozen between 800 and 2,200K. The translational temperature falls to 500K in the nozzle exit, and the different rotational temperatures experience a small departure from equilibrium, ranging from as low as 500K to as high as 800K.

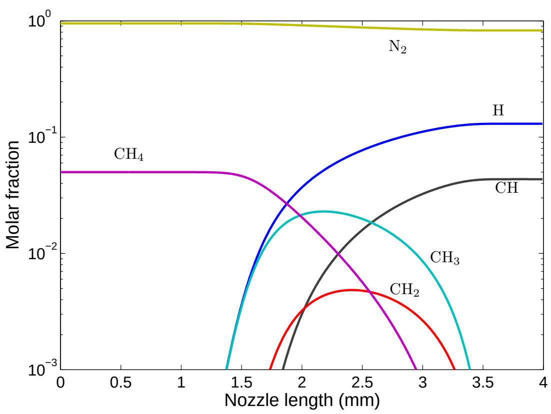

Fig. 7: Chemical Species Molar Fractions in the Nozzle Throat Region, for a N_2–CH_4 mixture

The measured spectra of the CN Violet system have been fitted using the SPARTAN code. As it has previously been acknowledged [4], the vibrational levels do not follow a Boltzmann distribution. Each vibrational level relative population has been iterated until a best fit was achieved. An additional parameter to be iterated in the fit is the rotational temperature, as a Boltzmann distribution of the rotational levels is experimentally determined to be established. The spectral constants and Einstein coefficients utilized in the spectral simulation have been taken from Ref. [3].

For the CN spectra issued from the the N_2–CH_4 plasma, the fitting can be ambiguous. If a Boltzmann equilibrium for the vibrational levels is assumed, a quite reasonable fit can be achieved considering T_v=T_r=10,000K, if some un-fitted lines are discarded as a background noise. However, as such values are very unlikely at the nozzle exit, a more careful fit was tried, without assuming that the vibrational levels follow a Boltzmann distribution. The newer fit is achieved for T_r=2,700K, with a slightly improved reproduction of the experimentally-measured spectrum. These two proposed fits are presented in Fig. 8

Similarly, the best achieved fit for the CO_2–N_2 plasma is presented in Fig. 9. The fitted rotational temperature is T_r=3,700K.

The comparison of the simulated and experimentally determined rotational temperatures of CN shows inconclusive results. For the CO_2–N_2 plasma, the predicted rotational temperature of CN is T_r=4,700K, whereas the measured temperature is T_r=3,700K, 1,000K below. For the N_2–CH_4 plasma, the predicted rotational temperature of CN is T_r=800K, whereas the measured temperature is T_r=2,700K, more than 2,000K above.

3.2 Comparison of Measured and Simulated N_2^+ Populations for Different Power Budgets of an Air Plasma

For an Air mixture with a mass flow rate of 0.40 g/s, five input arc plasma discharge powers are considered (4.25kW, 5.15kW, 6.97kW, 8.63kW, 10.4kW) for the same pressure in the gas arrival circuit (39900Pa) and for the same static pressure in the vacuum chamber (5.3Pa). For this range of increasing powers, the specific enthalpy is growing from 5.3MJ/kg to 16.2MJ/kg and the global efficiency of the arc discharge from 49% to 62% (see Tab. 3). These different operating points have been simulated using the TNeC code. A sample calculation is presented for Case 4 of Tab. 3 in Fig. 10.

The behavior of the different temperatures T, T_r, T_v in the arc-jet is similar for Earth and Mars atmospheres. In the nozzle throat exit, the translational

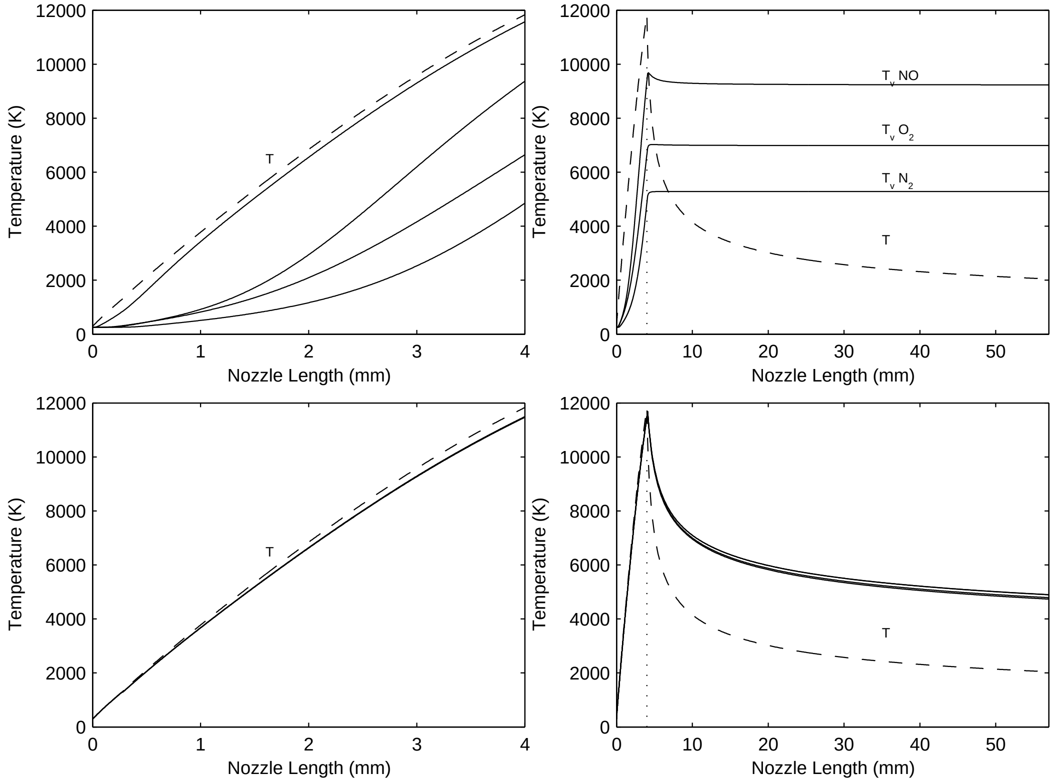

Fig. 10: Vibrational (Top) and Rotational (Bottom) Temperatures of the Molecular Species in the Nozzle Throat (Left) and Diverging Section (Right), for an Air Mixture

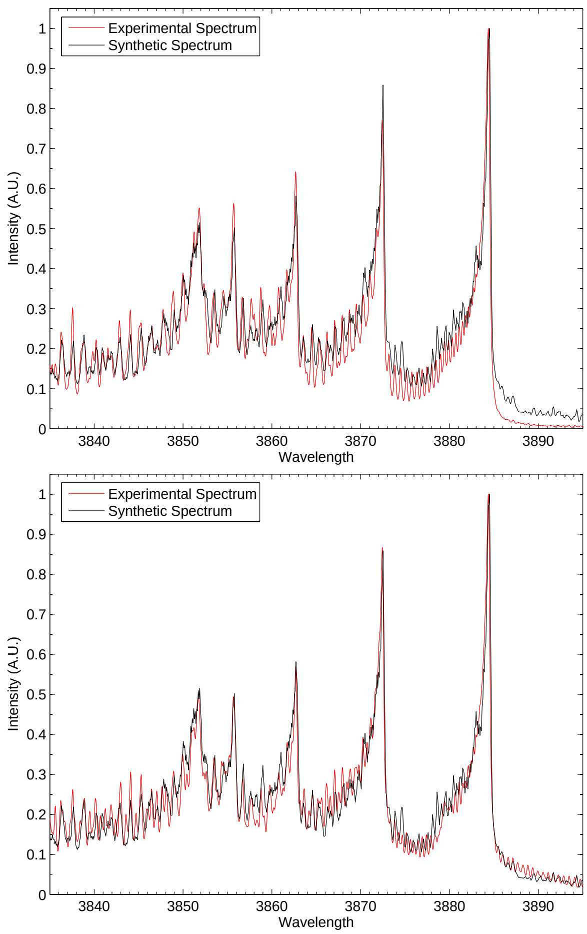

Fig. 8: Fitting of the CN Violet Spectra, Assuming a Boltzmann distribution of the internal levels at $T_{v,r}$=10,000K(top), and assuming a nonequilibrium distribution of the vibrational levels, with T_r=2,700K (bottom), for a N_2–CH_4 mixture

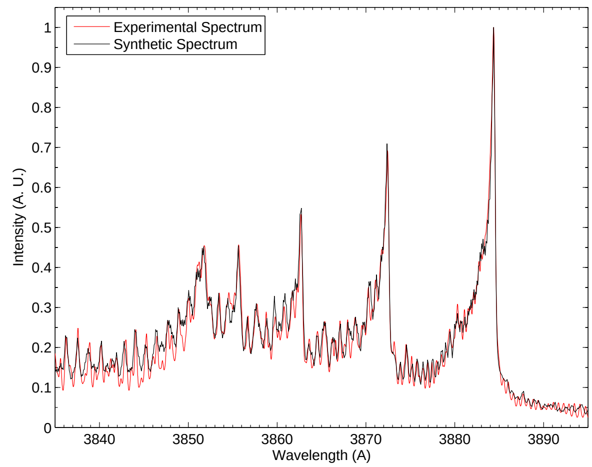

Fig. 9: Fitting of the CN Violet Spectra, Assuming a nonequilibrium distribution of the vibrational levels, with T_r=3,700K, for a CO_2–N_2 mixture

temperature T is more important reaches 11,000K. As usual, rotation stays in equilibrium with translation in the nozzle throat, with the vibrational temperatures rising slowly enough that V–T equilibrium is not reached in the nozzle throat exit. In the diverging section, translational temperature falls down to 2,000K at the nozzle exit, with the rotational temperatures relaxating more slowly to 5,000K. The vibrational temperatures for N_2, O_2 and NO become frozen in the diverging region at respectively around 5,000K, 7,000K, and 9,000K.

For air plasmas, the selected radiative system is the N_2^+ First Negative System, centered around 3900Åfor $\Delta v = 0$. Unlike CN, the vibrational bands for this system are more largely spaced, which means that only the 0–0 and 1–1 bands can be probed in the spectrometer spectral region. As for CN, the Abel–inverted spectra have been numerically fitted using the SPARTAN code, for each of the operating points of the air plasma. A sample calculation, carried out for case 2 of air show a best fit at T_v=2,000Kand T_r=5,000K. The comparison between simulation and experiment is presented in Fig. 11.

This procedure has been repeated for each oper-

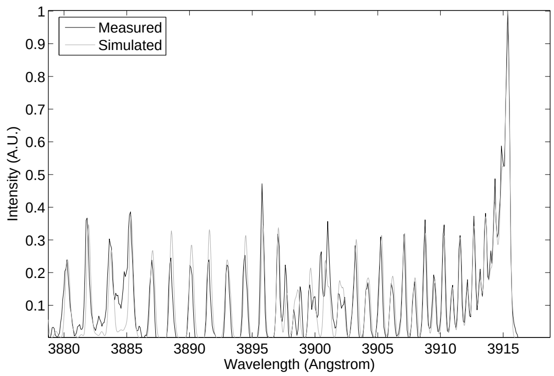

Fig. 11: Fitting of the N_2^+ 1st Negative Spectra, Assuming a Boltzmann distribution of the internal levels at T_v=2,000Kand T_r=5,000K

ating case of the air plasma. The fitted vibrational and rotational temperatures can then be calculated against the calculated temperatures predicted by the TNeC code in the nozzle exit, as a function of the arc power. The comparison is presented in Fig. 12.

The obtained results show that as it would be expected, the experimental and numerical vibrational temperatures differ sensibly. Indeed it is likely that similarly to the CN Violet System, the N_2^+ First Negative System vibrational mode does not follow a Boltzmann equilibrium distribution. This can only be speculated though, given that only the populations of the v=0 and v=1 levels can be probed. On the other hand, the predicted rotational temperatures, although slightly below the measured ones, follow closely the increasing thrend as the arc power input increases. This shows once again that, although the models implemented in the TNeC code are too simple for it to represent a robust enough predictive tool, the obtained results allow obtaining valuable information on the evolution of the exchange processes among the different molecules translational and internal modes.

References

[1] Lino da Silva M., "An Adaptive Line-by-Line-Statistical Model for Fast and Accurate Spectral Simulations in Low-Pressure Plasmas", *Journal of Quantitative Spectroscopy and Radiative Transfer*, Vol. 108, No. 1, 2007, pp. 106-125.

[2] *http://cfp.ist.utl.pt/radiation/*

[3] Lino da Silva M., and Dudeck M., "Arrays of Radiative Transition Probabilities for CO2-N2 Plasmas", *Journal of Quantitative Spectroscopy and Radiative Transfer*, Vol. 102, No. 3, 2006, pp. 348-386.

[4] Lino da Silva M., "Simulation des Propriétés Radiatives du Plasma Entourant un Véhicule Traversant une Atmosphère Planétaire à Vitesse Hypersonique: Application à la planète Mars", PhD Thesis (in French), *Université. Orléans*, 2004.

[5] Mazouffre S., Caubet-Hilloutou V., Lengrand J. C., and Pawelec E., "Examination of the Shock Wave Regular Reflexion Phenomenon in a Rarefied Supersonic Plasma Flow", *Phys. Plasmas*, Vol. 12, 2005, pp. 012323.

[6] Mazouffre S., and Pawelec E., "Metastable Oxygen Atom Velocity and Temperature in Supersonic CO_2 Plasma Expansions", *J. Phys D*, Vol. 42, 2009, pp. 015203.

[7] Lino da Silva M., Passarinho F., and Dudeck M., "Modeling of a CO_2-N_2 Plasma Flow in a Supersonic Arcjet Facility", *Journal of Thermophysics and Heat Transfer*, Vol. 20, No. 4, 2006, pp. 680–688.

[8] Shatalov O. P., and Losev S. A., "Modeling of Diatomic Molecules Dissociation Under Quasistationary Conditions", *AIAA Paper 97–2579*, 1997.

[9] Park C., "Nonequilibrium Hypersonic Aerothermodynamics", *John Wiley & Sons, Inc.*, New-York, 1989.

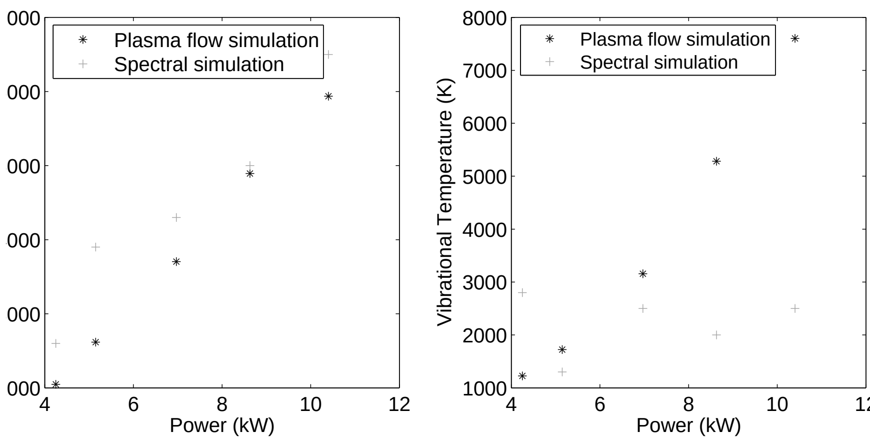

Fig. 12: Comparison of experimentally-determined and calculated rotational (left) and vibrational (right) temperatures in the nozzle exit, for an air plasma with different arc powers

[10] Parker J. G., "Rotational and Vibrational Relaxation in Diatomic Gases", *Physics of Fluids*, Vol. 2, No. 4, pp. 449–462, 1959.

[11] Millikan R. C., and White D. R., "Systematics of Vibrational Relaxation", *Journal of Chemical Physics*, Vol. 39, No. 12, pp. 3209–3213, 1963.

[12] Park C., "Review of Chemical-Kinetic Problems of Future NASA Missions, I: Earth Entries", *Journal of Thermophysics and Heat Transfer*, Vol. 7, No. 3, pp. 385–398, 1993.

[13] Losev S. A., Kozlov P. V., Kuznetsova L. A., Makarov V. N., Romanenko Yu. V., Surzhikov S. T., and Zalogin G. N., "Radiation of Mixture CO_2–N_2–Ar in Shock Waves: Experiment and Modelling", *Third European Symposium on Aerothermodynamics for Space Vehicles*, 1998.

[14] Park C., Howe J. T., Jaffe R. L., and Candler G. V., "Review of Chemical-Kinetic Problems of Future NASA Missions, II: Mars Entries", *Journal of Thermophysics and Heat Transfer*, Vol. 8, No. 1, 1994, pp. 9–23.

[15] Gokcen T., "N_2-CH_4-Ar Chemical Kinetic Model for Simulations of Atmospheric Entry to Titan", *Journal of Thermophysics and Heat Transfer*, Vol. 21, No. 1, 2007 pp. 9–18.